MATHEMATICAL MODELING AND COMPUTING, Vol. 6, No. 2, pp. 297–303 (2019)

Influence of the electroneutrality of a metal layer on the plasmon spectrum in dielectric–metal–dielectric structures

Kostrobij P. P., Markovych B. M., Polovyi V. Ye.

Lviv Polytechnic National University,
12 S. Bandera Str., 79013, Lviv, Ukraine

(Received 20 May 2019; Revised 11 November 2019; Accepted 15 November 2019)

In this paper, we propose a model that allows us to investigate the influence of quantum size effects and the electroneutrality condition on the spectrum of SPPs waves as a function of metal thickness in heterogeneous dielectric/metal/dielectric structures. It is shown that for ultrathin metal layers, the spectrum of plasmon waves has oscillatory behavior in the domain of small wave vectors ($k \approx 0.05-0.2\,\mathrm{nm}^{-1}$). The amplitude of oscillations depends on the conditions of electroneutrality for the dielectric/metal/dielectric structure.

Keywords: *surface plasmon, plasmon spectrum, metal layer thickness, dielectric permittivity, electroneutrality.*

2000 MSC: 78A50, 78-05, 78A25

UDC: 537.5.8:535.5:519.6 **DOI:** 10.23939/mmc2019.02.297

1. Introduction

Investigation of the properties of atomically thin metal films (ATMF) is attracting increasing attention [1–3]. It is because such scales quantum size effects the characteristics of ATMF begin to affect quite significantly [4]. Obviously, the mentioned effects should affect the behaviour of a spectrum of plasmon waves in dielectric/ATMF/dielectric structures. The evidence of this is the results of experiments published in [6, 7]. Therefore, considering all the above, a problem of constructing a mathematical model to describe the influence of quantum size effects on a spectrum of plasmon waves for ATMF is of current interest and needs consideration.

In this paper, we propose to improve the model [8] taking into account the electroneutrality condition [3,4,9] and to investigate its influence on the dependence of the plasmon spectrum on a thickness of ATMF.

2. Problem formulation

The mathematical model of plasmonic waves propagation in a heterogeneous (dielectric/ATMF/dielectric) structure (Fig. 1) is analogous to the one obtained in the previous work [8]. In this model, dielectric permittivities ε_1 and ε_3 of insulators are functions of the time variable t

$$\varepsilon_1 = \varepsilon_1(t), \quad \varepsilon_3 = \varepsilon_3(t), \tag{1}$$

and the dielectric permittivity of ATMF

$$\varepsilon_2 = \varepsilon_2(\boldsymbol{r}_{||}, z, t), \quad \boldsymbol{r}_{||} = (x, y), \tag{2}$$

depends on both t and spatial coordinates $\boldsymbol{r}_{||}$, z (geometry of the structure).

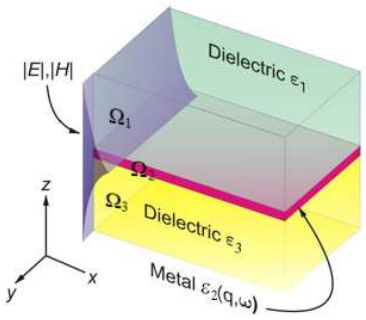

Fig. 1. Geometry of the structure.

We assume that there are no external charges ρ in the contact region between dielectrics and ATMF. In this case, the system of Maxwell's equations [10, 11] is such:

$$\begin{gathered} \nabla \cdot \boldsymbol{D} = \rho = 0, \quad \nabla \cdot \boldsymbol{B} = 0, \\ \nabla \times \boldsymbol{E} = \rho = 0, \quad \nabla \times \boldsymbol{H} = \boldsymbol{J} + \frac{\partial \boldsymbol{D}}{\partial t}, \end{gathered} \tag{3}$$

where $\boldsymbol{D}$ is electric flux density, $\boldsymbol{B}$ is magnetic flux density, $\boldsymbol{E}$ is electric field strength, $\boldsymbol{H}$ is magnetic field strength, $\boldsymbol{J}$ is external electric current density. Here "$\cdot$" is the dot product, "$\times$" is the cross product. Also, we assume that non-local interconnection between $\boldsymbol{E}$ and $\boldsymbol{D}$ [11] vectors exists:

$$\boldsymbol{D}(\boldsymbol{r}_{||},z,t)=\iiint d\boldsymbol{r}'_{||}\,dz'\,dt'\,\varepsilon_i(\boldsymbol{r}_{||}-\boldsymbol{r}'_{||},z,z',t-t')\,\boldsymbol{E}(\boldsymbol{r}'_{||},z',t'),\quad i=1,2,3. \tag{4}$$

Taking into account (1) and (2), we model the permittivity in areas of the structure (see Fig. 1) as follows

$$\begin{aligned}
&\varepsilon_1(\boldsymbol{r}_{||}-\boldsymbol{r}'_{||},z,z',t-t')=\varepsilon_1(t-t')\,\delta(\boldsymbol{r}_{||}-\boldsymbol{r}'_{||})\,\delta(z-z'),\\
&\varepsilon_2(\boldsymbol{r}_{||}-\boldsymbol{r}'_{||},z,z',t-t')=\varepsilon_2(\boldsymbol{r}_{||}-\boldsymbol{r}'_{||},z,t-t')\,\delta(z-z'),\\
&\varepsilon_3(\boldsymbol{r}_{||}-\boldsymbol{r}'_{||},z,z',t-t')=\varepsilon_3(t-t')\,\delta(\boldsymbol{r}_{||}-\boldsymbol{r}'_{||})\,\delta(z-z'),
\end{aligned} \tag{5}$$

where $\delta(z)$ is the Dirac delta function [15]. By defining the Fourier transform with respect to time

$$f(t)=\frac{1}{2\pi}\int_{-\infty}^{\infty}\tilde{f}(\omega)\,e^{i\omega t}\,d\omega,\quad \tilde{f}(\omega)=\int_{-\infty}^{\infty}f(t)\,e^{-i\omega t}\,dt, \tag{6}$$

we will obtain the following expression for $\varepsilon_i(\boldsymbol{r}_{||}-\boldsymbol{r}'_{||},z,z',t-t')$:

$$\varepsilon_i(\boldsymbol{r}_{||}-\boldsymbol{r}'_{||},z,z',t-t')=\frac{\Omega}{(2\pi)^3}\int_{-\infty}^{\infty}d\omega\int_{\Omega}d\boldsymbol{k}\,\varepsilon_i(\boldsymbol{k},z,z',\omega)\,e^{-i(\boldsymbol{k},\boldsymbol{r}_{||}-\boldsymbol{r}'_{||})-i\omega(t-t')}, \tag{7}$$

where $\Omega=\mathbb{R}^2$ is the domain of the 2D vector $\boldsymbol{k}=(k_x,k_y)$.

As before [8], we will consider the case of the transverse magnetic (TM) polarization of $\boldsymbol{E}$ and $\boldsymbol{H}$ vectors, for which [10]

$$\begin{aligned}
&\boldsymbol{E}=(E_x,0,E_y),\quad \boldsymbol{H}=(0,H_y,0),\\
&\boldsymbol{H}(\boldsymbol{r},\omega)=\boldsymbol{H}(z,\omega)\,e^{ik_xx},
\end{aligned}$$

k_x is the wave vector in the direction of propagation. For the TM polarization from Maxwell's equations (3) we obtain the following system of wave equations for $\boldsymbol{H}$ [10]

$$\frac{\partial^2H_y(z,\omega)}{\partial z^2}+\big(k_0^2\varepsilon_1(\omega)-k_x^2\big)H_y(z,\omega)=0, \tag{8}$$

$$\frac{\partial^2H_y(z,\omega)}{\partial z^2}+\big(k_0^2\varepsilon_2(\boldsymbol{k},z,\omega)-k_x^2\big)H_y(z,\omega)=0, \tag{9}$$

$$\frac{\partial^2H_y(z,\omega)}{\partial z^2}+\big(k_0^2\varepsilon_3(\omega)-k_x^2\big)H_y(z,\omega)=0, \tag{10}$$

$k_0=\omega/c$, c is the speed of light in a vacuum. Further investigation of this system requires simulation of dielectric permittivities $\varepsilon_1(\omega)$, $\varepsilon_2(\boldsymbol{k},z,\omega)$, $\varepsilon_3(\omega)$.

3. Modeling of dielectric permittivity of ATMF

Consider the dielectric permittivities ε_1 and ε_3, we can limit ourselves to the high-frequency approximation [10], namely, put that

$$\begin{aligned}
&\varepsilon_1(\boldsymbol{r}_{||}-\boldsymbol{r}'_{||},z,z',t-t')=\varepsilon_0\varepsilon_1(+\infty)\,\delta(t-t')\,\delta(\boldsymbol{r}_{||}-\boldsymbol{r}'_{||})\,\delta(z-z'),\\
&\varepsilon_3(\boldsymbol{r}_{||}-\boldsymbol{r}'_{||},z,z',t-t')=\varepsilon_0\varepsilon_3(+\infty)\,\delta(t-t')\,\delta(\boldsymbol{r}_{||}-\boldsymbol{r}'_{||})\,\delta(z-z'),
\end{aligned} \tag{11}$$

where ε_0 is dielectric permittivity of vacuum, $\varepsilon_{1,3}(+\infty)=\text{const}$ is high-frequency dielectric constant, but to model the dielectric function of ATMF we use the approach proposed in [8].

We model ATMF by a system of non-interacting electrons in an asymmetric rectangular potential well of finite width. In addition, we will only take into account spatial dispersion along Z axis, therefore $\boldsymbol{r}_{||} - \boldsymbol{r}'_{||} = 0$. In this case, the function $\varepsilon_2(\boldsymbol{r}_{||} - \boldsymbol{r}'_{||}, z, z', \omega)$ built of the diagonal components of the dielectric permittivity tensor has the form [1]

$$\varepsilon_2(0, z, z', \omega) = \varepsilon_2(z, \omega)\,\delta(z - z') = \left(1 - \frac{\omega_p^2}{\pi n_e \omega^2} \sum_{n=1}^{n_{max}} (k_F^2 - \alpha_n^2)|\phi_n(z)|^2\right)\delta(z - z'). \tag{12}$$

Here $\omega_p = \sqrt{4\pi n_e e^2/m_e}$ is the plasma frequency [10, 12], n_e is an electron density in ATMF [12], k_F is the Fermi wave vectors [12, 14], α_n is quantum numbers of bound states. The presence of surfaces is described by the potential

$$U(z) = \begin{cases} U_1, & \text{if} \quad z \leqslant 0, \\ 0, & \text{if} \quad 0 < z < L_{well}, \\ U_2, & \text{if} \quad z \geqslant L_{well}. \end{cases} \tag{13}$$

Here L_{well} is a width of the potential well. The function

$$\psi_n(\boldsymbol{r}) = \sqrt{\frac{2}{S}}\, e^{i(\boldsymbol{k}\cdot\boldsymbol{r}_{||})}\, \phi_n(z). \tag{14}$$

is the wave function [15] of an electron in ATMF, $\phi_n(z)$ is the solution of the Schrödinger stationary equation [2, 4, 13, 15]

$$-\frac{\hbar^2}{2m}\frac{d^2}{dz^2}\phi_n(z) + U(z)\,\phi_n(z) = W\phi_n(z), \tag{15}$$

with the Dirichlet boundary conditions

$$\lim_{z \to \pm\infty} \phi_n(z) = 0. \tag{16}$$

The solution of (15) with the potential (13) has the following form [4]:

$$\phi_n(z) = C(\alpha) \begin{cases} \dfrac{\alpha}{s_1} e^{\sqrt{s_1^2 - \alpha^2}\, z}, & \text{if} \quad z \leqslant 0, \\ \sin\left(\alpha z + \arcsin\dfrac{\alpha}{s_1}\right), & \text{if} \quad 0 < z < L_{well}, \\ \sin\left(\alpha L_{well} + \arcsin\dfrac{\alpha}{s_1}\right) e^{-\sqrt{s_2^2 - \alpha^2}(z - L_{well})}, & \text{if} \quad z \geqslant L_{well}, \end{cases} \tag{17}$$

where $s_i = \sqrt{2mU_i}/\hbar$, $i = 1, 2$, $C(\alpha)$ is the normalising constant [4]

$$C(\alpha) = \frac{\sqrt{2}}{\sqrt{L_{well} + \frac{(\alpha/s_1)^2}{\sqrt{s_1^2 - \alpha^2}} + \frac{(\alpha/s_2)^2}{\sqrt{s_2^2 - \alpha^2}} - \frac{1}{\alpha}\sin\left(\alpha L_{well}\right)\cos\left(\alpha L_{well} + 2\arcsin\frac{\alpha}{s_1}\right)}}. \tag{18}$$

To find quantum numbers α_n we need to solve the equation [2, 4, 13]:

$$\alpha_n L_{well} = \pi n - \arcsin\frac{\alpha_n}{s_1} + \arcsin\frac{\alpha_n}{s_2}, \tag{19}$$

the maximum number of bound states n_{max} we will find from the condition [4]

$$n_{max} = \left[\frac{1}{\pi}\left(L_{well}\min(s_1, s_2) + \arcsin\frac{\min(s_1, s_2)}{s_1} + \arcsin\frac{\min(s_1, s_2)}{s_2}\right)\right],$$

where "$[\cdot]$" is the ceiling function.

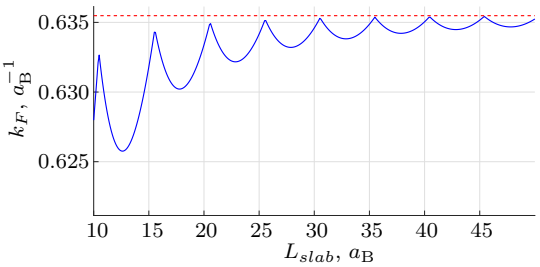

Fig. 2. The Fermi wave vector as a function of the film thickness. The dotted horizontal curve shows the bulk Fermi wave vector.

In this paper, we consider two models for describing a potential well: (a) the bulk chemical potential is used as the chemical potential of ATMF; (b) the chemical potential of ATMF is calculated as in [4]. In the second (b) case, it is stated that the width of the potential well depends on the penetration of electrons into the dielectric, namely [4] $L_{well} = L_{slab} + d_1 + d_2$, where L_{slab} is a geometric thickness of ATMF and d_i is determined from the condition of electroneutrality and according to [5]

$$d_i = \frac{3\pi}{8k_F} + \frac{\pi^2}{8k_F^2 L_{well}} - \frac{3}{4k_F}\left(\sqrt{\frac{s_i^2}{k_F^2} - 1} + \left(2 - \frac{s_i^2}{k_F^2}\right)\arcsin\frac{k_F}{s_i}\right), \quad i = 1, 2. \tag{20}$$

The Fermi wave vector k_F is unknown and should be determined from the electroneutrality condition [4]

$$\frac{2}{3r_s^3} = \frac{1}{L_{slab}}\sum_{n=1}^{n_{max}}(k_F^2 - \alpha_n^2), \tag{21}$$

In this case, the width of the well also depends on a concentration of electrons. The difference between the Fermi wave vectors in both cases is depicted in (Fig. 2).

4. Dispersion relation and plasmon spectrum simulation results

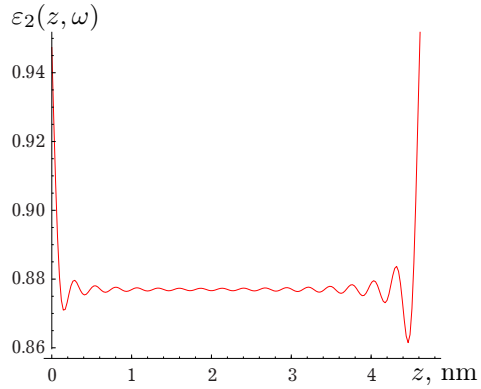

Fig. 3. Dielectric permittivity of ATMF $L_{slab} = 5\,\text{nm}$ when frequency $\frac{\omega}{\omega_p} = 4$.

In Fig. 3, the behaviour of $\varepsilon_2(z,\omega)$ is depicted. From this figure it is seen that the dielectric function $\varepsilon_2(z,\omega)$ differs from a constant only near the dielectric/ATMF and ATMF/dielectric interfaces. Let us assume that

$$\varepsilon_2(z,z',\omega) = \big(\varepsilon_2(L_{well},\omega) + \eta\,\Delta\varepsilon_2(z,\omega)\big)\,\delta(z-z'),$$

where

$$\varepsilon_2(L_{well},\omega) = \frac{1}{L_{well}}\int_0^{L_{well}}\varepsilon_2(z,\omega)\,dz = 1 - \frac{\omega_p^2}{2\pi n_e\omega^2}\sum_{n=1}^{n_{max}}(k_F^2 - k_n^2)\overline{|\phi_n(z)|}^2, \tag{22}$$

$$\overline{|\phi_n(z)|}^2 = \frac{1}{L_{well}}\int_0^{L_{well}}|\phi_n(z)|^2 dz \tag{23}$$

and $\Delta\varepsilon_2(z,\omega)$ are terms that describe behaviour $\varepsilon_2(z,\omega)$ in near-surface areas, η is the small parameter. Taking this into account, we represent the solution of the equation (9) for $H_y(z,\omega)$ as series in powers of η

$$H_y(z,\omega) = \sum_{m=0}^{\infty}\eta^m H_m(z,\omega) \tag{24}$$

and obtain the equation for $H_0(z,\omega)$ and $H_1(z,\omega)$:

$$\frac{\partial^2 H_0(z,\omega)}{\partial z^2} + \big(k_0^2\varepsilon(L_{well},\omega) - k_x^2\big)H_0(z,\omega) = 0, \tag{25}$$

$$\frac{\partial^2 H_1(z,\omega)}{\partial z^2} + \left(k_0^2 \varepsilon(L_{well},\omega) - k_x^2\right) H_1(z,\omega) = -k_0^2\,\eta\,\Delta\varepsilon(z,\omega)\,H_0(z,\omega). \tag{26}$$

As in [8], when finding the influence of the thickness L_{slab} of ATMF on the plasmon spectrum, we limit ourselves to the case $H_y(z,\omega) \approx H_0(z,\omega)$. In this case, the dispersion relation for finding the spectrum has the form

$$e^{-4k_1\frac{L_{well}}{2}} = \frac{k_1/\varepsilon_1 + k_2/\varepsilon_2}{k_1/\varepsilon_1 + k_2/\varepsilon_2}\,\frac{k_3/\varepsilon_1 + k_3/\varepsilon_2}{k_3/\varepsilon_3 + k_2/\varepsilon_2}, \qquad k_i^2 = k_x^2 - k_0^2\,\varepsilon_i, \quad i = 1,2,3 \tag{27}$$

that coincides with results obtained in [10]. Here $\varepsilon_1 = \varepsilon(\omega)$, $\varepsilon_2 = \varepsilon(\omega, L_{well})$, $\varepsilon_3 = \varepsilon(\omega)$.

The dielectric function of ATMF is described by the function (14)

$$\varepsilon_2(L_{well},\omega) = 1 - \frac{\omega_p^2}{2\pi n_e \omega^2} \sum_{n=1}^{n_{max}} (k_F^2 - k_n^2)\overline{|\phi_n(z)|}^2. \tag{28}$$

The simulation was carried out for the parameters that correspond to the structures Vacuum/Ag/Al_2O_3, SiO_2/Ag/Al_2O_3, Vacuum/Ag/Si (Table 1). All these parameters we took from [3,9] and from [6] for Ag on Si substrate.

Table 1. The parameters of the structures considered in the simulation.

Structure	ε_1	ε_2	U_1, eV	U_2, eV
Vacuum/Ag/Al_2O_3	1	9	9.855	8.505
SiO_2/Ag/Al_2O_3	4	9	8.755	8.505
Vacuum/Ag/Si	1	13	9.855	5.805

Fig. 4 shows results for "relatively great" thicknesses of ATMF (1000 ÷ 1020 Bohr radius) that was compared with the Drude model with negligible damping [10] for Vacuum/Ag/Al_2O_3,

$$\varepsilon(\omega, L_{well}) = \varepsilon_D(\omega) = 1 - \frac{\omega_p^2}{\omega} \tag{29}$$

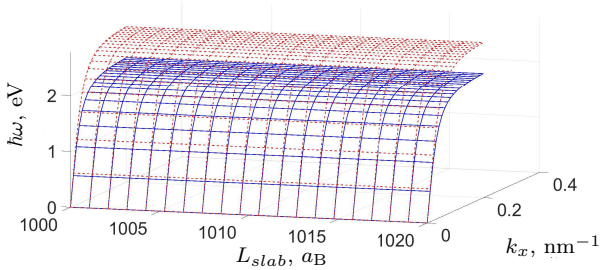

Fig. 4. Dependence of the plasmon spectrum on the ATMF thickness for the structure Vacuum/Ag/Al_2O_3 in two cases: for the Drude model ($\varepsilon_D(\omega)$) (dotted curves), for $\varepsilon_2(L_{well},\omega)$ (solid lines).

Figs. 5–7 show the results of simulation for the structures Vacuum/Ag/Al_2O_3, SiO_2/Ag/Al_2O_3 and Vacuum/Ag/Si for ATMFs $\sim 10 \div 50$ nm thick in Bohr radius.

Table 2 shows the results of comparison with [6] (column Exp.) for Vacuum/Ag/Si structure when $L_{slab} \approx 2.4$ nm or ≈ 43.54 Bohr radius. Unfortunately, in [6] data are presented only for small wave vectors ($k_x \lessapprox 0.1\,\text{nm}^{-1}$). Nevertheless, we can see that with increasing of the wave vector k_x, the difference between simulation and experiment increases too. As we mentioned before, for Vacuum/Ag/Si structure there is almost no difference between two considered models. But still, we have provided data for both models.

Table 2. Comparison with the experiment for Vacuum/Ag/Si structure for $L_{slab} \approx 2.4$ nm.

$k_x \approx 0.028\,\text{nm}^{-1}$				$k_x \approx 0.049\,\text{nm}^{-1}$			
k_x	(a)	(b)	Exp.	k_x	(a)	(b)	Exp.
0.02731	1.272	1.272	0.62	0.04824	1.774	1.776	0.8
0.02753	1.279	1.280	0.62	0.04847	1.778	1.780	0.8
0.02776	1.287	1.288	0.62	0.04870	1.781	1.784	0.8
0.02799	1.294	1.295	0.62	0.04892	1.785	1.787	0.8
0.02822	1.302	1.303	0.62	0.04915	1.789	1.791	0.8
0.02844	1.309	1.310	0.62	0.04938	1.792	1.795	0.8
0.02867	1.316	1.317	0.62	0.04961	1.796	1.798	0.8

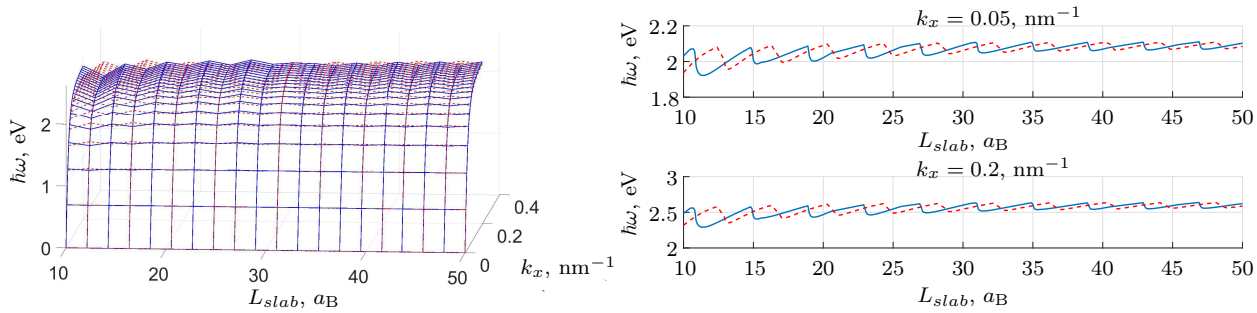

Fig. 5. Dependence of the plasmon spectrum on the ATMF thickness for the structure Vacuum/Ag/Al_2O_3 in the cases (a) (dotted curves) and (b) (solid curves).

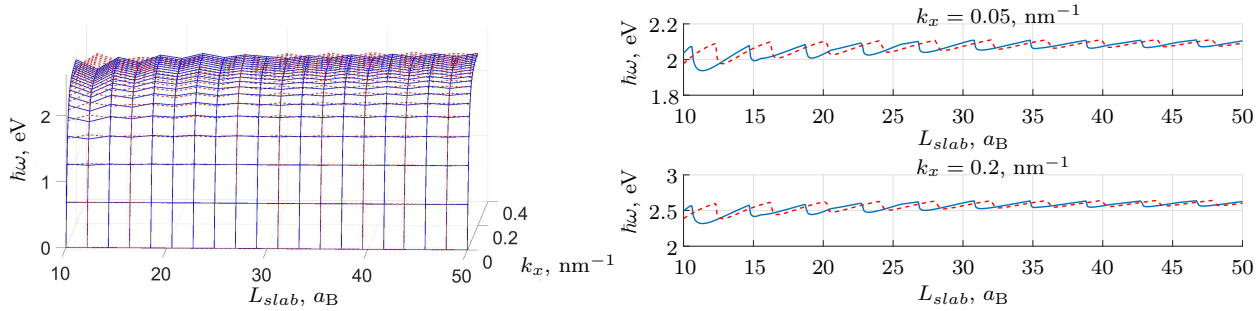

Fig. 6. Dependence of the plasmon spectrum on the ATMF thickness for the structure SiO_2/Ag/Al_2O_3 in the cases (a) (dotted curves) and (b) (solid curves).

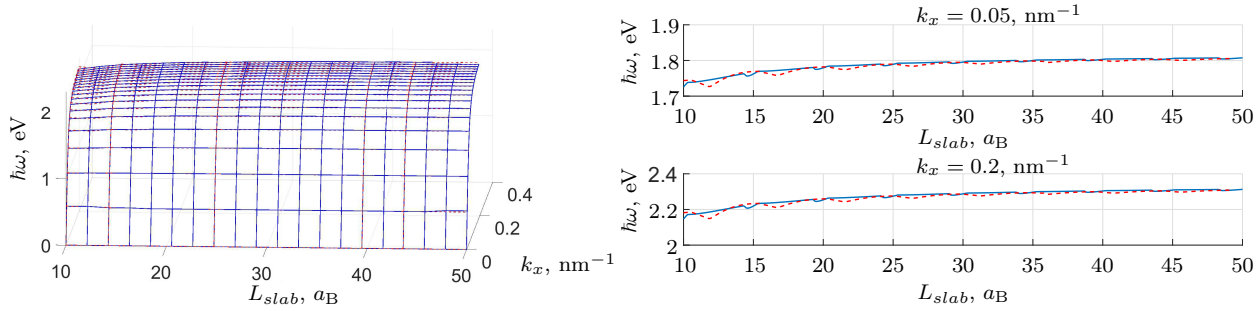

Fig. 7. Dependence of the plasmon spectrum on the ATMF thickness for the structure Vacuum/Ag/Si in the cases (a) (dotted curves) and (b) (solid curves).

5. Conclusions

The conducted analysis shows that for films with a thickness of $\sim 10 \div 20$ ML, the influence of quantum effects is noticeable when wave vector $k_x \gtrapprox 0.1\,\text{nm}^{-1}$ [2, 4]. The dependence of the plasmon spectrum on the film thickness has a distinct oscillating character for Vacuum/Ag/Al_2O_3, SiO_2/Ag/Al_2O_3 sandwiches with a gradual decrease in the amplitude of oscillations with increasing thickness. But for Vacuum/Ag/Si oscillations are much less observable.

Taking into account the discreteness of the Fermi wave vector and the conditions of electroneutrality for small thicknesses gives the shift of the oscillation peaks with a general tendency towards a decrease in the plasmon spectrum frequency peaks compared with the case when the wave vector depends only on a concentration of electrons in ATMF for Vacuum/Ag/Al_2O_3, SiO_2/Ag/Al_2O_3. For Vacuum/Ag/Si the difference between two models almost negligible. Also, there is significant dependence of the spectrum on the dielectric media surrounding ATMF. For "relatively thick" films, the difference between the models becomes less noticeable, and both charts slowly approach the Drude model from below.

[1] Kurbatsky V. P. Dielectric tensor of low-dimensional metal systems. J. Exp. Theor. Phys. **125** (1), 148–158 (2017).

[2] Kostrobij P. P., Markovych B. M. Effect of Coulomb interaction on chemical potential of metal film. Philosophical Magazine. **98** (21), 1991–2002 (2018).

[3] Korotun A. V. Size Oscillations of the Work Function of a Metal Film on a Dielectric Substrate. Phys. Solid State. **57** (2), 391–394 (2015).

[4] Kostrobij P. P., Markovych B. M. The chemical potential and the work function of a metal film on a dielectric substrate. Philosophical Magazine Letters. **99** (1), 12–20 (2019).

[5] van Himbergen J. E., Silbey R. Exact solution of metal surface properties in square barrier and linear one-electron potential models. Phys. Rev. B. **18** (6), 2674–2682 (1978).

[6] Abd El-Fattah Z. M., Mkhitaryan V., Brede J., Fernández L., Li C., Guo Q., Ghosh A., Echarri A. R., Naveh D., Xia F., Ortega J. E., de Abajo F. J. G. Plasmonics in Atomically-Thin Crystalline Silver Films. ACS Nano. **13** (7), 7771–7779 (2019).

[7] Echarri A. R., Cox J. D., de Abajo F. J. G. Quantum Effects in the Acoustic Plasmons of Atomically-Thin Heterostructures. Optica. **6** (5), 630–641 (2019).

[8] Kostrobij P. P., Polovyi V. Y. Surface plasmon polaritons in dielectric/metal/dielectric structures: metal layer thickness influence. Mathematical Modeling and Computing. **6** (1), 109–115 (2019).

[9] Pogosov V. V., Babich A. V., Vakula P. V. On the Influence of the Band Structure of Insulators and Image Forces on the Spectral Characteristics of Metal–Insulator Film Systems. Phys. Solid State. **55** (10), 2120–2123 (2013).

[10] Maier S. A. Plasmonics: Fundamentals and Application. Springer, New York (2007).

[11] Jackson J. D. Classical Electrodynamics. John Wiley & Sons (2007).

[12] Ashcroft N. W, Mermin N. D. Solid State Physics. Harcourt College Publishers (1976).

[13] Landau L. D., Bell J. S., Kearsley M. J, Pitaevskii L. P, Lifshitz E. M., Sykes J. B. Electrodynamics of Continuous Media. Elsevier, Vol. 8 (1984).

[14] Landau L. D., Lifshitz E. M. Statistical Physics. Elsevier, Vol. 5 (2013).

[15] Vakarchuk I. O. Kvantova mekhanika. Lviv, LNU im. I. Franka (2007), (in Ukrainian).

Вплив електронейтральності металевого прошарку на плазмонний спектр у структурах "діелектрик–метал–діелектрик"

Костробій П. П., Маркович Б. М., Польовий В. Є.

Національний університет "Львівська політехніка", вул. С. Бандери, 12, Львів, 79013, Україна

У роботі запропоновано модель, яка дає змогу дослідити вплив квантоворозмірних ефектів та умови електронейтральності на спектр SPPs хвиль як функції товщини металу в гетерогенних структурах "діелектрик–метал–діелектрик". Показано, що для надтонких металевих прошарків спектр плазмонних хвиль проявляє осциляційну поведінку в області малих хвильових векторів ($k \approx 0.05 - 0.2\,\text{нм}^{-1}$). Амплітуда осциляцій залежить від умов електронейтральності для структури "діелектрик–метал–діелектрик".

Ключові слова: *поверхневий плазмон, спектр плазмона, товщина металевого шару, діелектрична проникність, електронейтральність.*

2000 MSC: 78A50, 78-05, 78A25

УДК: 537.5.8:535.5:519.6